



Power Electronic Systems
Laboratory

© 2012 IEEE

IEEE Transactions on Industrial Electronics Vol. 58, No. 11, pp. 4986-4987, September 2012.

Imposed Sinusoidal Source and Load Currents for an Indirect Matrix Converter

M. Rivera
J. Rodriguez
J. R. Espinoza
T. Friedli
J. W. Kolar
A. Wilson
C. A. Rojas

This material is posted here with permission of the IEEE. Such permission of the IEEE does not in any way imply IEEE endorsement of any of ETH Zurich's products or services. Internal or personal use of this material is permitted. However, permission to reprint/republish this material for advertising or promotional purposes or for creating new collective works for resale or redistribution must be obtained from the IEEE by writing to pubs-permissions@ieee.org. By choosing to view this document, you agree to all provisions of the copyright laws protecting it.



Eidgenössische Technische Hochschule Zürich
Swiss Federal Institute of Technology Zurich

Imposed Sinusoidal Source and Load Currents for an Indirect Matrix Converter

Marco Rivera, *Member, IEEE*, Jose Rodriguez, *Fellow, IEEE*, José R. Espinoza, *Member, IEEE*, Thomas Friedli, *Member, IEEE*, Johann W. Kolar, *Fellow, IEEE*, Alan Wilson, *Member, IEEE*, and Christian A. Rojas, *Student Member, IEEE*

Abstract—A new strategy for indirect matrix converters which allows an optimal control of source and load currents is presented in this paper. This method uses the commutation state of the converter in the subsequent sampling time according to an optimization algorithm given by a simple cost functional and the discrete system model. The control goals are regulation of output current according to an arbitrary reference and also a good tracking of the source current to its reference which is imposed to have a sinusoidal waveform with low distortion. Experimental results support the theoretical development.

Index Terms—AC–AC power conversion, current control, matrix converter, predictive control.

NOMENCLATURE

\mathbf{i}_s	Source current $[i_{sA} \ i_{sB} \ i_{sC}]^T$.
\mathbf{v}_s	Source voltage $[v_{sA} \ v_{sB} \ v_{sC}]^T$.
\mathbf{i}_i	Input current $[i_A \ i_B \ i_C]^T$.
\mathbf{v}_i	Input voltage $[v_A \ v_B \ v_C]^T$.
\mathbf{i}_o	Load current $[i_a \ i_b \ i_c]^T$.
\mathbf{v}_o	Load voltage $[v_a \ v_b \ v_c]^T$.
\mathbf{i}_s^*	Source current reference $[i_{sA}^* \ i_{sB}^* \ i_{sC}^*]^T$.
\mathbf{i}_o^*	Output current reference $[i_a^* \ i_b^* \ i_c^*]^T$.
C_f	Filter capacitor.
L_f	Filter inductor.
R_f	Filter resistor.
R_L	Load resistance.
L_L	Load inductance.

I. INTRODUCTION

THE indirect matrix converter (IMC) [1] has been the subject of investigation for some time. One of the favorable features of an IMC is the absence of a dc-link capaci-

tor, which allows for the construction of compact converters capable of operating at adverse atmospheric conditions such as extreme temperatures and pressures. These features have been explored extensively and are the main reasons why the matrix converters family has been investigated for decades [2]. IMC features an easy to implement and more secure commutation technique, the dc-link zero current commutation [3]. Moreover, the conventional IMC has bidirectional power flow capabilities and can be designed to have small sized reactive elements in its input filter. These characteristics make the IMC a suitable technology for high-efficiency converters for specific applications such as military, aerospace, wind turbine generator system, external elevators for building construction and skin pass mill, as reported in [4]–[6], where these advantages make up for the additional cost of an IMC compared to conventional converters. IMC uses complex pulse width modulation (PWM) and space vector modulation (SVM) schemes to achieve the goal of unity power factor and sinusoidal output current [2], [7]–[13]. Thanks to technological advances, fast and powerful microprocessors are used for the control and modulation of power converters. To deal with the high processing power needed for these microprocessors, some research has shown the positive potential of model predictive control (MPC) techniques in many power electronics applications [14], [15]. This is a nonlinear control method that takes advantage of the discrete inherent nature of the commutated power converter. While there are a few challenges to the predictive control method, it has been demonstrated as an appealing alternative to power converter control because its concepts are very intuitive and easy to understand, and it can be applied to a wide variety of systems. In addition, it may involve multiple systems, dead time compensation, and nonlinear constraints, making it an easy controller to implement, particularly since it is open to modifications and extensions for specific applications, as reviewed in [16]–[21]. This control scheme has some advantages over traditional linear controllers and PWM modulators, such as fast dynamic responses and an easy inclusion of constraints on the system [22]. Predictive current control (PCC) can be described as a particular case of MPC which takes into account the inherent discrete nature of the switching states of the power converter and the digital implementation [20], [21], [23]–[25]. Most of PCC methods applied in matrix converters take into consideration the output current regulation and the instantaneous reactive power minimization on the input side, obtaining input currents in phase with their respective phase voltages. However, this cannot ensure that they present a sinusoidal

Manuscript received October 9, 2010; revised July 4, 2011; accepted October 3, 2011. Date of publication October 14, 2011; date of current version April 13, 2012. This work was supported by the Centro Científico-Tecnológico de Valparaíso (CCTVal) No. FB0821, FONDECYT Project, under Grant 1100404 and by the Universidad Técnica Federico Santa María.

M. Rivera, J. Rodriguez, A. Wilson, and C. A. Rojas are with the Electronics Engineering Department, Universidad Técnica Federico Santa María (UTFSM), 2390123 Valparaíso, Chile (e-mail: marco.rivera@usm.cl; jrp@usm.cl; alan.wilson@usm.cl; christian.rojas@usm.cl).

J. R. Espinoza is with the Department of Electrical Engineering, Universidad de Concepción, 407-0386 Concepción, Chile (e-mail: jose.espinoza@udec.cl).

T. Friedli and J. W. Kolar are with the Power Electronic Systems Laboratory, Swiss Federal Institute of Technology (ETH) Zurich, 8092 Zurich, Switzerland (e-mail: thomas.friedli@ieee.org; kolar@lem.ee.ethz.ch).

Color versions of one or more of the figures in this paper are available online at <http://ieeexplore.ieee.org>.

Digital Object Identifier 10.1109/TIE.2011.2172171

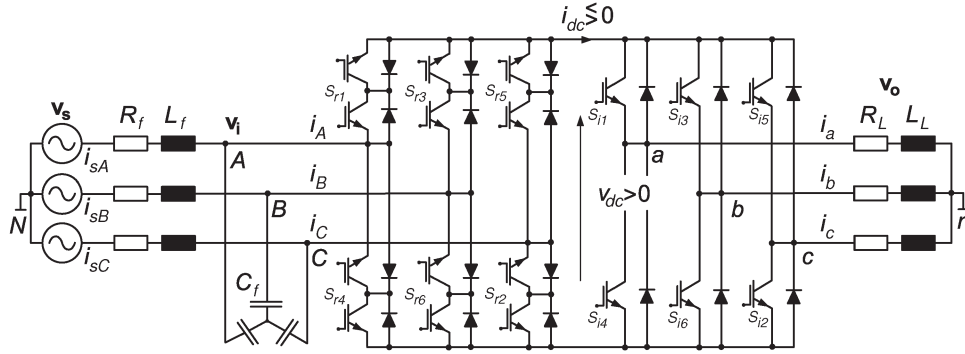


Fig. 1. General topology of the 3×3 indirect matrix converter.

waveform, particularly when harmonic distortion is present in the source voltage. To overcome this issue and enhance the quality of the source current, in the following pages, this paper illustrates how the PCC can be applied to an IMC and how both source and load currents waveforms can be directly controlled.

II. INDIRECT MATRIX CONVERTER MODEL

The IMC topology is shown in Fig. 1. DC-link voltage v_{dc} is obtained as a function of the rectifier switches and the input voltages \mathbf{v}_i as follows:

$$v_{dc} = [S_{r1} - S_{r4} \quad S_{r3} - S_{r6} \quad S_{r5} - S_{r2}] \mathbf{v}_i \quad (1)$$

and input currents \mathbf{i}_i are defined as a function of the rectifier switches and the dc-link current i_{dc} as

$$\mathbf{i}_i = \begin{bmatrix} S_{r1} - S_{r4} \\ S_{r3} - S_{r6} \\ S_{r5} - S_{r2} \end{bmatrix} i_{dc}. \quad (2)$$

DC-link current i_{dc} is determined as a function of the inverter switches and the output currents \mathbf{i}_o as

$$i_{dc} = [S_{i1} \quad S_{i3} \quad S_{i5}] \mathbf{i}_o \quad (3)$$

and finally, output voltages are synthesized as a function of the inverter switches and the dc-link voltage v_{dc} as

$$\mathbf{v}_o = \begin{bmatrix} S_{i1} - S_{i4} \\ S_{i3} - S_{i6} \\ S_{i5} - S_{i2} \end{bmatrix} v_{dc}. \quad (4)$$

These equations correspond to the nine and eight valid switching states for the rectifier and the inverter stage, respectively, as reported in [3], following the restrictions of no short circuits in the input and no open lines in the output. A positive dc-link voltage at any time is also mandatory for a conventional IMC, so the nine rectifier states reduce to only three valid states in every sampling time T_s . In addition, the rectifier includes an $L_f C_f$ filter on the input side which is needed to prevent over voltages and to provide filtering of the high-frequency components of the input currents produced by

the commutations and the inductive nature of the load. The filter consists of a second-order system described by

$$\frac{d\mathbf{i}_s}{dt} = \frac{1}{L_f} (\mathbf{v}_s - \mathbf{v}_i) - \frac{R_f}{L_f} \mathbf{i}_s \quad (5)$$

$$\frac{d\mathbf{v}_i}{dt} = \frac{1}{C_f} (\mathbf{i}_s - \mathbf{i}_i). \quad (6)$$

The load model is obtained similarly. Assuming an inductive-resistive load as shown in Fig. 1, the following equation describes the behavior of the load:

$$\frac{d\mathbf{i}_o}{dt} = \frac{1}{L_L} \mathbf{v}_o - \frac{R_L}{L_L} \mathbf{i}_o. \quad (7)$$

Additionally, the impedance model of the input filter is defined as

$$Z_c = \frac{1}{j\omega_s C_f} \quad (8)$$

$$Z_l = R_f + j\omega_s L_f \quad (9)$$

where $\omega_s = 2\pi f_s$, with f_s the source frequency. The load impedance is represented as

$$Z_o = R_L + j\omega_o L_L \quad (10)$$

where $\omega_o = 2\pi f_o$, with f_o the load frequency. Finally, the filter model in terms of impedance is given as

$$\begin{aligned} \mathbf{v}_s &= \mathbf{v}_i + \mathbf{i}_s Z_l \\ \mathbf{i}_s &= \mathbf{i}_i + \mathbf{v}_i / Z_c. \end{aligned} \quad (11)$$

III. PROBLEM ON THE INPUT SIDE

SVM and PWM techniques generate a desired output voltage with unity power factor [2], [7]–[13], but there is a displacement angle between the source line current \mathbf{i}_s and input current \mathbf{i}_i due to the filter parameters and consequently a displacement angle between the source voltage and current, requiring additional controllers to handle this angle [26]. From (8) and (9) and (11), this displacement angle is given as

$$\delta = \arctan(\omega_s C_f (V_s - R_f I_s)) / (I_s (1 - \omega_s^2 L_f C_f)) \quad (12)$$

where V_s and I_s are the source voltage and current fundamental amplitudes, respectively. In [26], it has been proposed that

space model [20], with the state variables \mathbf{i}_s and \mathbf{v}_i obtained from (5) and (6) as follows:

$$\begin{bmatrix} \dot{\mathbf{v}}_i \\ \dot{\mathbf{i}}_s \end{bmatrix} = \mathbf{A} \begin{bmatrix} \mathbf{v}_i \\ \mathbf{i}_s \end{bmatrix} + \mathbf{B} \begin{bmatrix} \mathbf{v}_s \\ \mathbf{i}_i \end{bmatrix} \quad (14)$$

where

$$\mathbf{A} = \begin{bmatrix} 0 & 1/C_f \\ -1/L_f & -R_f/L_f \end{bmatrix} \\ \mathbf{B} = \begin{bmatrix} 0 & -1/C_f \\ 1/L_f & 0 \end{bmatrix}. \quad (15)$$

The discrete time state space model is determined as

$$\begin{bmatrix} \mathbf{v}_i(k+1) \\ \mathbf{i}_s(k+1) \end{bmatrix} = \Phi \begin{bmatrix} \mathbf{v}_i(k) \\ \mathbf{i}_s(k) \end{bmatrix} + \Gamma \begin{bmatrix} \mathbf{v}_s(k) \\ \mathbf{i}_i(k) \end{bmatrix} \quad (16)$$

with

$$\Phi = e^{\mathbf{A}T_s}, \quad \Gamma = \mathbf{A}^{-1}(\Phi - \mathbf{I}_{2 \times 2})\mathbf{B}. \quad (17)$$

The output current prediction can be obtained using a forward Euler approximation in (7) as

$$\mathbf{i}_o(k+1) = d_1 \mathbf{v}_o(k) + d_2 \mathbf{i}_o(k) \quad (18)$$

where, $d_1 = T_s/L_L$ and $d_2 = 1 - R_L T_s/L_L$ are constants dependent on load parameters and the sampling time T_s [20]. Note that the current $\mathbf{i}_s(k+1)$ and $\mathbf{i}_o(k+1)$ depend upon $S_i(k)$ through (2) and (3).

B. Cost Function Definition

The error between the predicted load currents and its references can be expressed as follows:

$$\Delta i_o(k+1) = |i_{o\alpha}^* - i_{o\alpha}| + |i_{o\beta}^* - i_{o\beta}| \quad (19)$$

where $i_{o\alpha}$ and $i_{o\beta}$ denote the load current in $\alpha\beta$ coordinates for $k+1$ sample time, and $i_{o\alpha}^*$ and $i_{o\beta}^*$ their respective references. Furthermore, the error between the reference and predicted value of the source current can be expressed as

$$\Delta i_s(k+1) = |i_{s\alpha}^* - i_{s\alpha}| + |i_{s\beta}^* - i_{s\beta}| \quad (20)$$

where, $i_{s\alpha}^*$ and $i_{s\beta}^*$ correspond to the source current references (see Appendix for additional information) and $i_{s\alpha}$ and $i_{s\beta}$ are the source current predictions in sample $k+1$. Expressions of (19) and (20) are merged in a single cost function as indicated in (21) which is evaluated for every switching state, applying to the converter the switching state that minimizes this quality function, as has been explained before. Finally, (19) and (20) are combined into a single so-called quality function as follows:

$$g = \Delta i_o(k+1) + \gamma_i \Delta i_s(k+1) \quad (21)$$

where γ_i is a weighting factor. Noting that $g=0$ (for an arbitrary value of γ_i) gives perfect tracking of the load and source currents, then by minimizing g , the optimum value for

TABLE I
EXPERIMENTAL SETUP PARAMETERS

Variables	Description	Value
T_s	Sampling time	20 μ s
V_s	Supply phase voltage	105V
f_s	Supply frequency	50Hz
L_f	Input filter inductance	5.9mH
C_f	Input filter capacitance	10 μ F
R_f	Input filter resistance	0.5 Ω
R_L	Load resistance	10 Ω
L_L	Load inductance	15mH
f_o	Output frequency	50Hz
λ_i	Weighting factor	20
λ_q	Weighting factor	0.003
I_o^*	Output current reference	4.50A
I_s^*	Input current reference	2.11A

commutation state is guaranteed. In practice, by the appropriate selection of the weighting factor γ_i , a given total harmonic distortion (THD) of the input and output currents is obtained. The principal method for selection of the weighting factors and analysis of the performance system effects is presented in [29], where first it is established in a value equal to zero to prioritize the control of the output current, and later it is increased slowly aiming to obtain minimal THD of source and load currents.

V. RESULTS

A laboratory IMC prototype designed and built by Universidad Tecnica Federico Santa Maria, thanks to the support of the Power Electronics Systems Laboratory of ETH Zurich, was used for experimental evaluation. The converter features insulated gate bipolar transistors (IGBTs) of type IXRH40N120 for the bidirectional switch of the rectifier side and standard IGBTs with antiparallel diodes IRG4PC30UD for the inverter stage. Experimental results are presented in this section, by considering the parameters indicated in Table I. As demonstrated in [3] and [15], the high calculation power of today's existing digital signal processors (DSPs) makes this method very attractive to control power converters. The control scheme presented in [3] was implemented in a 160 MIPS fixed point ADSP21991 DSP board and a sampling time of $T_s = 20 \mu$ s. In our experimental results, it has been considered the same sampling time, and the control scheme was implemented in a dSPACE 1103. Similar to the setup used in [3], the processor board is connected to additional boards that include a FPGA for the commutation sequence generation and the signal conditioning for the measurement of voltages and currents. In Section V-A, experimental results of the method proposed in [3] have been presented to compare them with experimental results of the proposed method which are presented in Section V-B. However, in this case, it is considered the utilization of a three-phase variac as the ac source available in our laboratory, which behaves like a weak ac supply for the system, due to the inductance associated with the autotransformer connection.

A. Method I: Predictive Current Control With Instantaneous Reactive Power Minimization

It is known that most industrial application requires unity power factor in the grid side. For this reason, as reported in

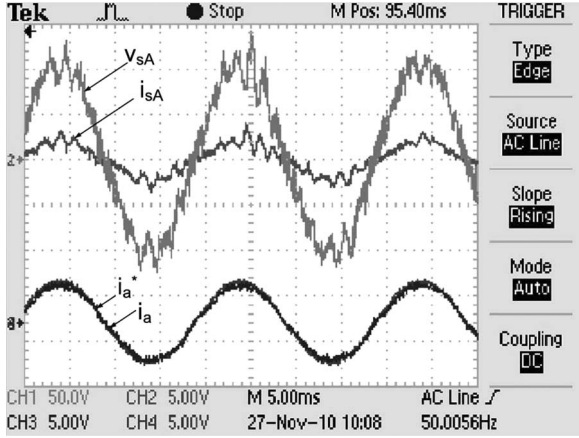


Fig. 3. Experimental results of current control with instantaneous reactive power minimization ($q_s^* = 0$); source voltage v_{sA} [V] and current i_{sA} [A]; output current i_a [A] and its reference i_a^* [A].

[3], through the instantaneous reactive power minimization, the system is forced to work with a unity DPF on the input side. The cost function considered in this case is

$$g = \Delta i_o^2 + \lambda_q \Delta q_s^2 \quad (22)$$

which allows the control of the load current and the minimization of the instantaneous reactive power on the input side. In (22), λ_q is a weighting factor, and Δq_s denotes the error between the reference and predicted value of the instantaneous reactive power in $k + 1$ sampling time, expressed as follows:

$$\Delta q_s = q_s^* - (v_{s\alpha} i_{s\beta} - v_{s\beta} i_{s\alpha}) \quad (23)$$

with $v_{s\alpha}$, $v_{s\beta}$, $i_{s\alpha}$, and $i_{s\beta}$ the source voltages and currents in $\alpha\beta$ coordinates, respectively. The instantaneous reactive power reference is established as $q_s^* = 0$ to have a unity DPF on the input side. Fig. 3 (above) shows the measured source current and voltage of phase A and Fig. 3 (below) shows the reference and measured output current of phase a . As expected, the source current fulfils the condition of unity DPF showing an almost sinusoidal waveform in phase with its respective voltage, and, as a consequence, the instantaneous reactive power is minimized.

This is achieved by considering the value of the weighting factor equal to $\lambda_q = 0.003$ which has been empirically adjusted as explained in [29], where first it is established in a value equal to zero to prioritize the control of the output current, and later it is increased slowly aiming to obtain unity DPF in the input currents while maintaining a good behavior on the output side. In Fig. 3, it is possible to observe a very good tracking of the load current i_a with respect to its reference i_a^* . As it can be observed in Fig. 3, the source current shows a ripple corresponding to the resonance frequency of the input filter and the harmonic distortion of the ac supply such as it can be observed in the spectrum of Fig. 4. This phenomenon is due to the utilization of a three-phase variac as the ac supply. A summary of the source current THD is given in Table II.

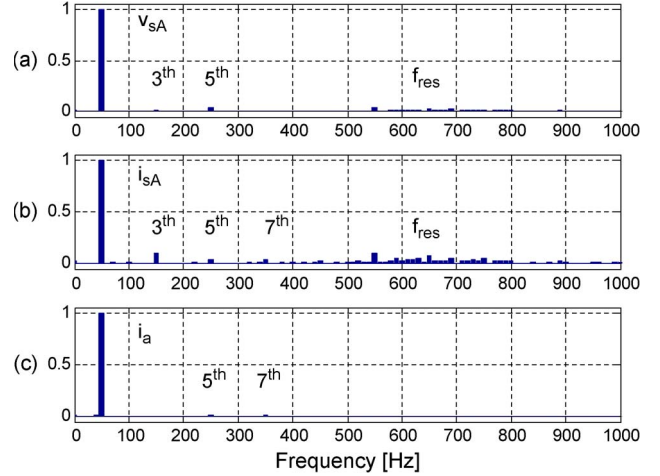


Fig. 4. Experimental results of current control including instantaneous reactive power minimization. (a) Spectrum of source voltage [pu]. (b) Spectrum of source current [pu]. (c) Spectrum of output current [pu].

TABLE II
EXPERIMENTAL THD RESULTS OF i_{sA}

reference	THD	3 th	5 th	7 th
$q_s^* = 0$	29.24%	9.88%	4.00%	3.89%
$i_s^*, \theta = 0$	21.17%	6.27%	1.51%	2.75%
$i_s^*, \theta = +30$	19.20%	5.23%	1.59%	1.66%
$i_s^*, \theta = -30$	19.64%	5.41%	2.77%	2.84%

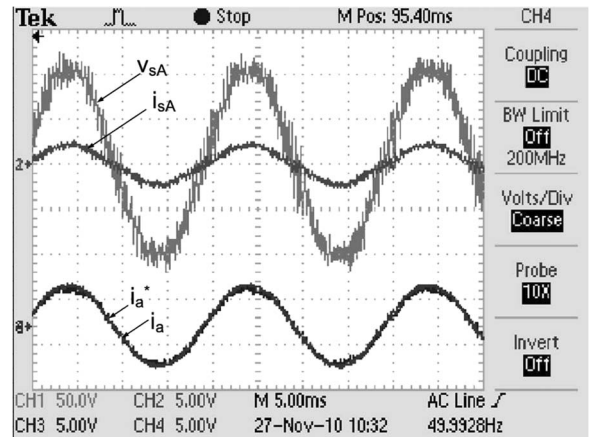


Fig. 5. Experimental results predictive control with imposed sinusoidal source ($\theta = 0$) and load currents; source voltage v_{sA} [V] and current i_{sA} [A]; output current i_a [A] and its reference i_a^* [A].

B. Method II: Predictive Current Control With Imposed Sinusoidal Source Currents

The proposed strategy is tested using the same parameters employed in Method I and detailed in Appendix—Table I. As mentioned before, the algorithm operates with a sample time of $T_s = 20 \mu s$.

The control strategy is evaluated considering the cost function indicated in (21) and with a weighting factor λ_i equal to $\lambda_i = 20$ which has been empirically adjusted as explained previously. In Fig. 5 is shown the source current i_{sA} and its respective source voltage v_{sA} , where the condition of zero DPF is fulfilled, which is imposed by the source current reference i_{sA}^* , being both source voltage and current in phase. Again, the

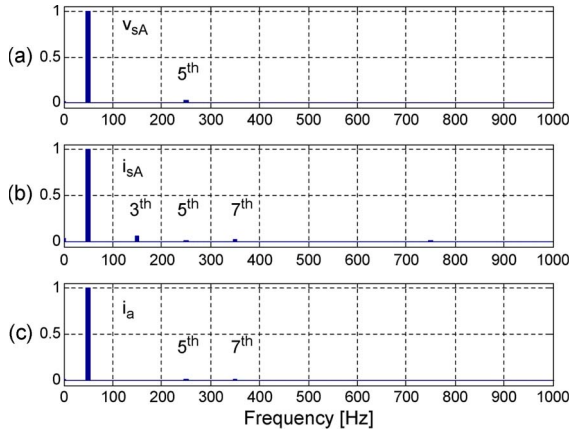


Fig. 6. Experimental results predictive control with imposed sinusoidal source ($\theta = 0$) and load currents. (a) Spectrum of source voltage [pu]. (b) Spectrum of source current [pu]. (c) Spectrum of output current [pu].

source current is forced to have a sinusoidal waveform with an amplitude of $I_s = 2.11$ A, independent of the distortion present in the source voltage or the input filter resonance. For this reason, the source current i_{sA} is almost sinusoidal and compared to the previous case (Figs. 3 and 4), the harmonic distortion and filter resonance are mitigated as demonstrated in Fig. 6(a) and (b). The cost that must be paid is high-frequency harmonics in both source current and voltage, but this issue is not considered in this paper. As it can be shown in Fig. 5, the source voltage is not completely clean because of the utilization of a three-phase variac as the ac source, which behaves like a weak ac supply for the system, due to the inductance associated with the autotransformer connection. On the output side, the load current i_a presents a good behavior with an almost sinusoidal waveform and 4.5 A of amplitude according to its reference as shown in Fig. 5. This method does not involve greater calculations, and it is immune to input filter resonances. With this idea, sinusoidal source and output currents can be obtained, realizing a desirable tracking to their respective references. To demonstrate the effectiveness of the proposed method and that the DPF can be easily handled, two tests have been done (Figs. 7 and 8) with a displacement of $\theta = 30^\circ$ and $\theta = -30^\circ$ between source voltage and current while maintaining the output current control. Again, the source voltage presents a harmonic distortion due to the ac supply utilized. Similarly, Figs. 9 and 10 show that the resonance of the input filter is mitigated. Our experimental results verified that it is possible to control both source and output currents at the same time, while keeping almost sinusoidal waveforms on both sides in spite of distortions or perturbations in the source voltage. A summary of the experimental THD is presented in Table II for all the cases presented in this paper. With the proposed method, it is possible to obtain a reduction of the THD in the source current with respect to the method proposed in [3]. It is expected that with a clean ac source, the input and output current THDs can be decreased.

VI. CONCLUSION

This paper has presented a predictive control method for a conventional IMC where the optimal control algorithm tests all

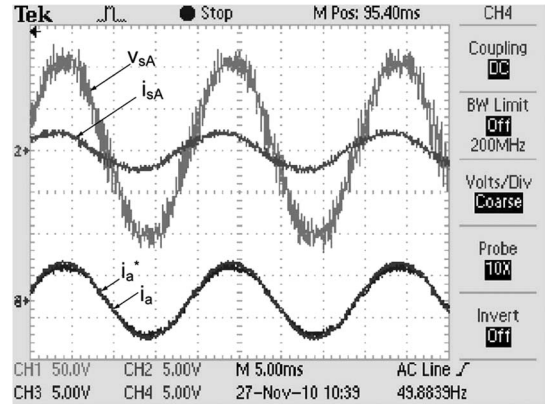


Fig. 7. Experimental results predictive control with imposed sinusoidal source ($\theta = +30$) and load currents; source voltage v_{sA} [V] and current i_{sA} [A]; output current i_a [A] and its reference i_a^* [A].

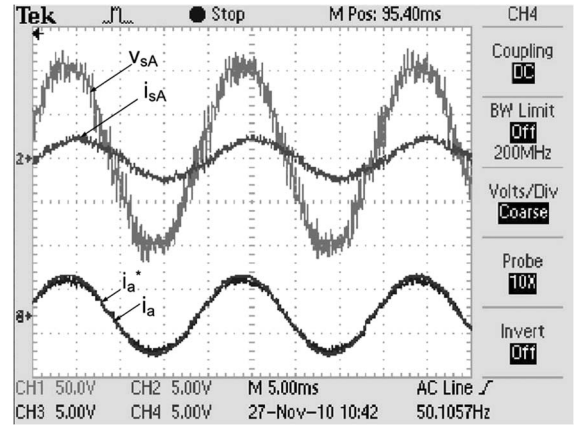


Fig. 8. Experimental results predictive control with imposed sinusoidal source ($\theta = -30$) and load currents; source voltage [50 V/div] and current [5 A/div]; output current and reference [5 A/div].

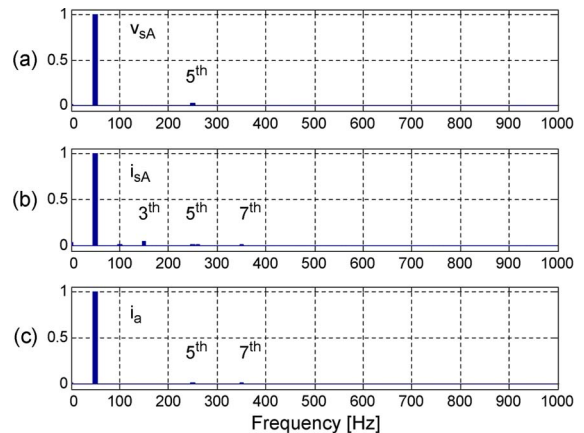


Fig. 9. Experimental results predictive control with imposed sinusoidal source ($\theta = +30$) and load currents. (a) Spectrum of source voltage [pu]. (b) Spectrum of source current [pu]. (c) Spectrum of output current [pu].

the 24 valid switching states of the converter at each sampling time and selects the one that minimizes a cost function. This function allows simultaneous control of source and output currents with sinusoidal waveforms, according to their references. Predictive control can prevent the need to use complex modulations techniques, internal cascade loops, and the gate

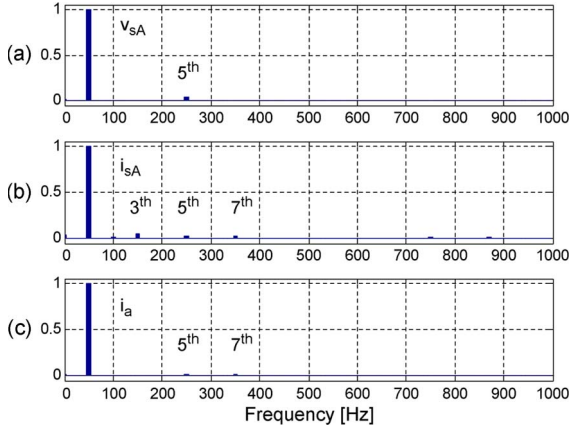


Fig. 10. Experimental results predictive control with imposed sinusoidal source ($\theta = -30$) and load currents. (a) Spectrum of source voltage [pu]. (b) Spectrum of source current [pu]. (c) Spectrum of output current [pu].

drive signals for the power switches are generated directly by the controller. Our experimental results indicate that the presented strategy provides good tracking of the source and output current to their references, making it possible to control both source and output currents at the same time, while keeping almost sinusoidal waveforms at both sides in spite of distortions or perturbations in the source voltage. Better results can be obtained by considering the use of a clean ac supply. The authors consider that in the future, deeper research must be done which must include more advanced aspects such as impedance variations, parameter adjustments, input filter design, and transients of the supply voltage and its effects, as well a complete assessment with respect to SVM in terms of switching losses, distortion, algorithms complexity, and others.

APPENDIX

A. Source Current Reference

From Fig. 1, the source voltage can be defined as

$$\begin{aligned} v_{sA} &= V_s \sin(\omega_s t) \\ v_{sB} &= V_s \sin(\omega_s t - 2\pi/3) \\ v_{sC} &= V_s \sin(\omega_s t + 2\pi/3). \end{aligned} \quad (24)$$

By using (11), it is possible to define the apparent power expression on the input side as follows:

$$S_{in} = V_i \cdot I_i \quad (25)$$

with V_i and I_i the instantaneous values of input voltage and current, respectively.

The real component of (25) corresponds to the input active power which is given as a function of the input side parameters as

$$P_i = \text{Re}\{S_{in}\} = 3I_s (1 - 8\pi^2 f_s^2 C_f L_f) (V_s - R_f I_s) \quad (26)$$

with I_s the fundamental source current amplitude, the value to be determined.

On the output side, the active power P_{out} is given as

$$P_{out} = 3R_L I_o^{*2} \quad (27)$$

with I_o the amplitude of the output current reference.

The relationship between the efficiency of the converter η , the input, and output active power is given as follows:

$$P_i \eta = P_o \quad (28)$$

which can be formulated in terms of the input and output variables of the converter and load current reference as

$$I_s (1 - 8\pi^2 f_s^2 C_f L_f) (V_s - R_f I_s) \eta = R_L I_o^{*2}. \quad (29)$$

Equation (29) can be expressed as

$$(\lambda V_s I_s - \lambda R_f I_s^2) \eta = R_L I_o^{*2} \quad (30)$$

by considering $\lambda = 1 - 8\pi^2 f_s^2 C_f L_f$. From (30), we can obtain a quadratic expression given as

$$-\lambda R_f I_s^2 + \lambda V_s I_s - \frac{R_L I_o^{*2}}{\eta} = 0. \quad (31)$$

Hence, from (31), it is possible to determine the fundamental source current amplitude as

$$I_s = \frac{-\lambda V_s \pm \sqrt{(\lambda V_s)^2 - 4\lambda R_f R_L I_o^{*2}/\eta}}{-2\lambda R_f}. \quad (32)$$

The source current amplitude is obtained as a function of the efficiency, the input filter parameters, the fundamental source voltage, and the amplitude of the output current reference. In addition, it is necessary to implement a phase-locked-loop to obtain the phase of the fundamental source voltage to generate the sinusoidal reference. Finally, the resulting source current reference is defined as

$$\begin{aligned} i_{sA}^* &= I_s \sin(\omega_s t + \theta) \\ i_{sB}^* &= I_s \sin(\omega_s t - 2\pi/3 + \theta) \\ i_{sC}^* &= I_s \sin(\omega_s t + 2\pi/3 + \theta) \end{aligned} \quad (33)$$

where θ is the parameter that allows a variable power factor, and it is considered equal to zero to obtain unity power factor.

B. Parameters and THD Information

The parameters of the experimental setup are indicated in Table I and the experimental THD information in Table II, respectively.

REFERENCES

- [1] T. Wijekoon, C. Klumpner, and P. Wheeler, "Implementation of a hybrid AC/AC direct power converter with unity voltage transfer ratio," in *Proc. 21st Annu. IEEE APEC*, 2006, p. 7.
- [2] J. Kolar, T. Friedli, F. Krismer, and S. Round, "The essence of three-phase AC/AC converter systems," in *Proc. 13th EPE-PEMC*, 2008, pp. 27–42.
- [3] P. Correa, J. Rodriguez, M. Rivera, J. Espinoza, and J. Kolar, "Predictive control of an indirect matrix converter," *IEEE Trans. Ind. Electron.*, vol. 56, no. 6, pp. 1847–1853, Jun. 2009.
- [4] P. Zanchetta, P. Wheeler, J. Clare, M. Bland, L. Empringham, and D. Katsis, "Control design of a three-phase matrix-converter-based ac/ac mobile utility power supply," *IEEE Trans. Ind. Electron.*, vol. 55, no. 1, pp. 209–217, Jan. 2008.

- [5] S. Lopez Arevalo, P. Zanchetta, P. Wheeler, A. Trentin, and L. Empringham, "Control and implementation of a matrix-converter-based ac ground power-supply unit for aircraft servicing," *IEEE Trans. Ind. Electron.*, vol. 57, no. 6, pp. 2076–2084, Jun. 2010.
- [6] E. Yamamoto, T. Kume, H. Hara, T. Uchino, J. Kang, and H. Krug, "Development of matrix converter and its applications in industry," in *Proc. 35th IEEE IECON*, Porto, Portugal, 2009, pp. 4–12.
- [7] X. Lu, K. Sun, G. Li, and L. Huang, "Analysis and control of input power factor in indirect matrix converter," in *Proc. 35th IEEE IECON*, 2009, pp. 207–212.
- [8] M. Jussila and H. Tuusa, "Comparison of simple control strategies of space-vector modulated indirect matrix converter under distorted supply voltage," *IEEE Trans. Power Electron.*, vol. 22, no. 1, pp. 139–148, Jan. 2007.
- [9] R. Pena, R. Cardenas, E. Reyes, J. Clare, and P. Wheeler, "A topology for multiple generation system with doubly fed induction machines and indirect matrix converter," *IEEE Trans. Ind. Electron.*, vol. 56, no. 10, pp. 4181–4193, Oct. 2009.
- [10] M. Y. Lee, P. Wheeler, and C. Klumpner, "Space-vector modulated multilevel matrix converter," *IEEE Trans. Ind. Electron.*, vol. 57, no. 10, pp. 3385–3394, Oct. 2010.
- [11] R. Cardenas-Dobson, R. Pena, P. Wheeler, and J. Clare, "Experimental validation of a space vector modulation algorithm for four-leg matrix converters," *IEEE Trans. Ind. Electron.*, vol. 58, no. 4, pp. 1282–1293, Apr. 2011.
- [12] T. Friedli and J. Kolar, "Comprehensive comparison of three-phase AC-AC matrix converter and voltage DC-link back-to-back converter systems," in *Proc. IPEC*, 2010, pp. 2789–2798.
- [13] J. Kolar, F. Schafmeister, S. Round, and H. Ertl, "Novel three-phase AC/AC sparse matrix converters," *IEEE Trans. Power Electron.*, vol. 22, no. 5, pp. 1649–1661, Sep. 2007.
- [14] S. Kouro, P. Cortes, R. Vargas, U. Ammann, and J. Rodriguez, "Model predictive control, a simple and powerful method to control power converters," *IEEE Trans. Ind. Electron.*, vol. 56, no. 6, pp. 1826–1838, Jun. 2009.
- [15] J. Rodriguez, J. Pontt, C. A. Silva, P. Correa, P. Lezana, P. Cortes, and U. Ammann, "Predictive current control of a voltage source inverter," *IEEE Trans. Ind. Electron.*, vol. 54, no. 1, pp. 495–503, Feb. 2007.
- [16] P. Correa, J. Rodriguez, I. Lizama, and D. Andler, "A predictive control scheme for current-source rectifiers," *IEEE Trans. Ind. Electron.*, vol. 56, no. 5, pp. 1813–1815, May 2009.
- [17] P. Cortes, G. Ortiz, J. Yuz, J. Rodriguez, S. Vazquez, and L. Franquelo, "Model predictive control of an inverter with output LC filter for UPS applications," *IEEE Trans. Ind. Electron.*, vol. 56, no. 6, pp. 1875–1883, Jun. 2009.
- [18] H. Miranda, P. Cortes, J. Yuz, and J. Rodriguez, "Predictive torque control of induction machines based on state-space models," *IEEE Trans. Ind. Electron.*, vol. 56, no. 6, pp. 1916–1924, Jun. 2009.
- [19] M. Preindl, E. Schaltz, and P. Thøgersen, "Switching frequency reduction using model predictive direct current control for high power voltage source inverters," *IEEE Trans. Ind. Electron.*, vol. 58, no. 7, pp. 2826–2835, Jul. 2011.
- [20] S. Muller, U. Ammann, and S. Rees, "New time-discrete modulation scheme for matrix converters," *IEEE Trans. Ind. Electron.*, vol. 52, no. 6, pp. 1607–1615, Dec. 2005.
- [21] R. Vargas, J. Rodriguez, U. Ammann, and P. Wheeler, "Predictive current control of an induction machine fed by a matrix converter with reactive power control," *IEEE Trans. Ind. Electron.*, vol. 55, no. 12, pp. 4362–4371, Dec. 2008.
- [22] P. Cortes, M. Kazmierkowski, R. Kennel, D. Quevedo, and J. Rodriguez, "Predictive control in power electronics and drives," *IEEE Trans. Ind. Electron.*, vol. 55, no. 12, pp. 4312–4324, Dec. 2008.
- [23] P. Cortes, J. Rodriguez, D. Quevedo, and C. Silva, "Predictive current control strategy with imposed load current spectrum," *IEEE Trans. Power Electron.*, vol. 23, no. 2, pp. 612–618, Mar. 2008.
- [24] J. Rodriguez, J. Kolar, J. Espinoza, M. Rivera, and C. Rojas, "Predictive current control with reactive power minimization in an indirect matrix converter," in *Proc. IEEE ICIT*, Mar. 2010, pp. 1839–1844.
- [25] M. Rivera, P. Correa, J. Rodriguez, I. Lizama, and J. Espinoza, "Predictive control of the indirect matrix converter with active damping," in *Proc. IEEE 6th IPEMC*, May 2009, pp. 1738–1744.
- [26] M. Nguyen, H. Lee, and T. Chun, "Input power factor compensation algorithms using a new direct-SVM method for matrix converter," *IEEE Trans. Ind. Electron.*, vol. 58, no. 1, pp. 232–243, Jan. 2011.
- [27] H. Nguyen, H.-H. Lee, and T.-W. Chun, "An investigation on direct space vector modulation methods for matrix converter," in *Proc. 35th IEEE IECON*, Nov. 2009, pp. 4493–4498.
- [28] J. Rodriguez, J. Kolar, J. Espinoza, M. Rivera, and C. Rojas, "Predictive torque and flux control of an induction machine fed by an indirect matrix converter with reactive power minimization," in *Proc. IEEE ISIE*, 2010, pp. 3177–3183.
- [29] P. Cortes, S. Kouro, B. La Rocca, R. Vargas, J. Rodriguez, J. Leon, S. Vazquez, and L. Franquelo, "Guidelines for weighting factors design in model predictive control of power converters and drives," in *Proc. IEEE ICIT*, Feb. 2009, pp. 1–7.



Marco Rivera (S'09–M'10) received the B.Sc. degree in electronics engineering, and the M.Sc. degree in electrical engineering from the Universidad de Concepción, Concepción, Chile, in 2007 and 2008, respectively, and the Ph.D. degree from the Department of Electronics Engineering, Universidad Técnica Federico Santa María (UTFSM), Valparaíso, Chile, in 2011.

During January and February of 2010, he was a visiting Ph.D. student of the Electrical and Computer Engineering Department, Ryerson University, Toronto, ON, Canada, where he worked on predictive control applied on four-leg inverters. He was also a visiting Ph.D. student at the Departamento de Ingeniería Eléctrica y Computacional de Instituto Tecnológico y de Estudios Superiores de Monterrey (ITESM), Monterrey, Mexico, where he worked on experimental aspects of a Double Fed Induction Generator—Indirect Matrix Converter System. Between September and November of 2011, he was a visiting Researcher in the Laboratoire PLASMA et Conversion d'Énergie, Université de Toulouse, Toulouse, France. He is currently working in a Postdoctoral position at UTFSM. His research interests include direct and indirect matrix converters, predictive and digital controls for high-power drives, four-leg converters, and development of high-performance control platforms based on field-programmable gate arrays.

Dr. Rivera was awarded a scholarship from the Marie Curie Host Fellowships for Early Stage Research Training in Electrical Energy Conversion and Conditioning Technology at University College Cork, Ireland in 2008.



Jose Rodriguez (M'81–SM'94–F'10) received the Engineer degree in electrical engineering from the Universidad Técnica Federico Santa María (UTFSM), Valparaíso, Chile, in 1977 and the Dr.-Ing. degree in electrical engineering from the University of Erlangen, Erlangen, Germany, in 1985.

He has been with the Department of Electronics Engineering, UTFSM since 1977, where he is currently full Professor and Rector. He has coauthored more than 300 journal and conference papers. His main research interests include multilevel inverters, new converter topologies, control of power converters, and adjustable-speed drives.

Dr. Rodriguez is member of the Chilean Academy of Engineering. He is an Associate Editor of the IEEE TRANSACTIONS ON POWER ELECTRONICS and IEEE TRANSACTIONS ON INDUSTRY ELECTRONICS since 2002. He received the Best Paper Award from the IEEE TRANSACTIONS ON INDUSTRY ELECTRONICS in 2007 and the Best Paper Award from the IEEE INDUSTRY ELECTRONICS MAGAZINE in 2008.



José R. Espinoza (S'92–M'97) received the Eng. degree in electronic engineering and the M.Sc. degree in electrical engineering from the University of Concepción, Concepción, Chile, in 1989 and 1992, respectively, and the Ph.D. degree in electrical engineering from Concordia University, Montreal, QC, Canada, in 1997.

Since 2006, he has been a Professor in the Department of Electrical Engineering, University of Concepción, where he is engaged in teaching and research in the areas of automatic control and power electronics. He has authored and coauthored more than 100 refereed journal and conference papers.

Dr. Espinoza is currently an Associate Editor of the IEEE TRANSACTIONS ON INDUSTRY ELECTRONICS and IEEE TRANSACTIONS ON POWER ELECTRONICS.



Thomas Friedli (M'09) received the M.Sc. degree in electrical engineering and information technology (with distinction) and the Ph.D. degree from the Swiss Federal Institute of Technology (ETH) Zurich, Zurich, Switzerland, in 2005 and 2010, respectively.

From 2003 to 2004, he worked as a trainee for Power-One in the RD center for telecom power supplies. His Ph.D. research from 2006 to 2009 involved the further development of current source and matrix converter topologies in collaboration with industry using silicon carbide JFETs and diodes and

a comparative evaluation of three-phase ac-ac converter systems.

Dr. Friedli received the First Prize Paper Award of the IEEE IAS IPCC in 2008 and the IEEE TRANSACTIONS ON INDUSTRY APPLICATIONS Prize Paper Award in 2009.



Johan W. Kolar (F'10) received the M.Sc. and Ph.D. degree (*summa cum laude/promotio sub auspiciis praesidentis rei publicae*) from the University of Technology Vienna, Vienna, Austria.

Since 1984, he has been working as an independent international consultant in close collaboration with the University of Technology Vienna, in the fields of power electronics, industrial electronics, and high-performance drives. He has proposed numerous novel converter topologies and modulation/control concepts, e.g., the VIENNA rectifier, the Swiss rectifier, and the three-phase ac-ac sparse matrix converter. He was appointed

Professor and Head of the Power Electronic Systems Laboratory at the Swiss Federal Institute of Technology (ETH) Zurich, Zurich, Switzerland, on February 1, 2001. He has published over 400 scientific papers in international journals and conference proceedings and has filed more than 80 patents. The focus of his current research is on ac-ac and ac-dc converter topologies with low effects on the mains, e.g., for data centers, More-Electric-Aircraft, and distributed renewable energy systems, and on Solid-State Transformers for Smart Microgrid Systems. Further main research areas are the realization of ultracompact and ultra-efficient converter modules employing latest power semiconductor technology (SiC and GaN), micropower electronics and/or Power Supplies on Chip, multidomain/scale modeling/simulation and multi-objective optimization, physical model-based lifetime prediction, pulsed power, and ultrahigh speed and bearingless motors.

Dr. Kolar is a member of the IEEJ and of International Steering Committees and Technical Program Committees of numerous international conferences in the field (e.g., Director of the Power Quality Branch of the International Conference on Power Conversion and Intelligent Motion). He is the founding Chairman of the IEEE PELS Austria and Switzerland Chapter and Chairman of the Education Chapter of the EPE Association. From 1997 through 2000, he has been serving as an Associate Editor of the IEEE TRANSACTIONS ON INDUSTRY ELECTRONICS and since 2001 as an Associate Editor of the IEEE TRANSACTIONS ON POWER ELECTRONICS. Since 2002, he also is an Associate Editor of the Journal of Power Electronics of the Korean Institute of Power Electronics and a member of the Editorial Advisory Board of the IEEJ Transactions on Electrical and Electronic Engineering. He received the Best Transactions Paper Award of the IEEE Industrial Electronics Society in 2005, the Best Paper Award of the ICPE in 2007, the First Prize Paper Award of the IEEE IAS IPCC in 2008, the IEEE IECON Best Paper Award of the IES PETC in 2009, the IEEE PELS Transaction Prize Paper Award 2009, the Best Paper Award of the IEEE/ASME TRANSACTIONS ON MECHATRONICS 2010, the IEEE PELS Transactions Prize Paper Award 2010, the Best Paper First Prize Award at the ECCE Asia 2011, and the First Place IEEE IAS Society Prize Paper Award 2011. He also received an Erskine Fellowship from the University of Canterbury, Christchurch, New Zealand, in 2003. He initiated and/or is the founder/cofounder of four spin-off companies targeting ultrahigh speed drives, multidomain/level simulation, ultracompact/efficient converter systems, and pulsed power/electronic energy processing. In 2006, the European Power Supplies Manufacturers Association awarded the Power Electronics Systems Laboratory of ETH Zurich as the leading academic research institution in Power Electronics in Europe.



Alan Wilson (M'10) received the B.S. and M.S. degrees in electronics engineering from the Universidad Técnica Federico Santa María (UTFSM), Valparaiso, Chile, in 2010.

From 2010 to 2011, he was a Scientific Assistant with the Department of Electronics Engineering, UTFSM. His research interests include multilevel voltage source inverters, predictive control of power converters, and development of control systems for power converters based on field-programmable gate array and DSPs.

Mr. Wilson was awarded a "Becas Chile" scholarship from the Chilean Research Foundation CONICYT in 2011 to pursue his Ph.D. degree in the Power Electronics Group, Technische Universität Dresden, Dresden, Germany.



Christian A. Rojas (S'10) received the Engineer degree in electronic engineering from the Universidad de Concepción, Concepción, Chile, in 2009.

His research interests include matrix converters, digital control, and model predictive control of power converters and drives.

Mr. Rojas was awarded a scholarship from the Chilean Research Foundation CONICYT in 2010 to pursue his Ph.D. studies in power electronics at Universidad Técnica Federico Santa María, Valparaiso, Chile.